

DETC98/MECH-5837

INTRODUCTION OF TWO-LINK, IN-PLANE, BISTABLE COMPLIANT MEMS

Brian D. Jensen

Mechanical Engineering
Department
Brigham Young University
Provo, Utah 84602
jensenb@et.byu.edu

Larry L. Howell

Mechanical Engineering
Department
Brigham Young University
Provo, Utah 84602
lhowell@et.byu.edu

Linton G. Salmon

Integrated Microelectronics
Laboratory
Electrical and Computer
Engineering Department
Brigham Young University
Provo, Utah 84602
linton_salmon@byu.edu

ABSTRACT

A bistable mechanism has two stable states within its range of motion. Its advantages include the ability to stay in two positions without power input and despite small external disturbances. Therefore, bistable micro-mechanisms could allow the creation of MEMS with improved energy efficiency and positioning accuracy. This paper presents the first bistable MEMS which function within the plane of fabrication. These bistable mechanisms, known as "Young" bistable mechanisms, obtain their energy storage characteristics from the deflection of two compliant members, have two pin joints connected to the substrate, and can be constructed of two layers of polysilicon. The pseudo-rigid-body model overcomes problems with nonlinearities in the analysis and design of these mechanisms. This approach allows greater freedom and flexibility in the design process. Testing of the mechanisms demonstrated their bistable behavior and the repeatability of the stable positions.

INTRODUCTION

This paper presents work on the development of a specific class of in-plane bistable MEMS. A bistable mechanism is a mechanism which has two stable equilibrium states within its range of motion. At these states, the mechanism requires no input power to remain in position, and the mechanism will return to its stable position after small disturbances. Because of their ability to stay in position without power input and regardless of external disturbances, bistable mechanisms can

allow MEMS systems to be built with increased energy efficiency and improved accuracy and precision in positioning. The energy efficiency effect may be especially critical in autonomous applications which must produce or store their own energy, such as devices which use micro-batteries as a power source. Bistable MEMS could also be used as mechanical switches, non-volatile memory, or micro-valves. They can also be used as micro-positioners with two repeatable positions. The mechanisms presented here demonstrate the design and fabrication of planar bistable MEMS and establish the repeatability of their stable positions.

Several examples of out-of-plane bistable mechanisms have been presented. Hälgl (1990) presented a bistable mechanism consisting of a flexible beam fixed at both ends. The beam was buckled up out of the plane of the substrate. By pulling on it with electrostatic forces, it was pulled into a second stable position curving down toward the substrate. A similar device was reported by Wagner et al. (1996). This device consisted of a curved membrane which could be pulled down toward the substrate using electrostatic forces. Matoba et al. (1994) fabricated a bistable mechanism which used thermal expansion as the actuating force. It consisted of a cantilever beam under compressive stress, so that the beam was buckled either down toward the substrate or up away from the substrate. The direction of buckling could be changed using thermal heating.

Each of these examples of bistable MEMS relies on buckling of beams or membranes to obtain bistable behavior. The advantage of this method is that it is simple and requires

less complex analysis. Trial and error approaches may even be used to find a working design of this type. However, lack of variety of possible motion, need for special fabrication, and reliance on residual stresses are all disadvantages of the buckling approach. The method used in this paper to design bistable devices provides more freedom and flexibility, allowing the designer to change the location of equilibrium points, the actuation force, and device stresses. Moreover, the mechanism designs require only simple and well-known surface micromachining processes for their fabrication.

The class of bistable MEMS studied here, known as “Young¹” mechanisms, overcomes other difficulties inherent to the design of planar bistable MEMS. For instance, bistable mechanisms must store and release energy during their motion (Opdahl et al., 1998). Young mechanisms, like all other previous bistable MEMS, use strain energy stored in flexible segments to gain bistable behavior as well as mechanism motion. These flexible segments must usually undergo large, nonlinear deflections, introducing high stresses and difficult nonlinear analysis. In addition, because an unstable position will always occur between two stable positions (Opdahl et al., 1998), finite element codes often become unstable while converging on solutions for these large deflections. Finally, the mechanism design must include considerations of the mechanism motion as well as the potential energy characteristics of the mechanism. Both mechanism motion and potential energy characteristics depend entirely on the configuration of the flexible segments within the mechanism, so that the designer must consider both issues simultaneously. Young mechanisms allow the designer to use contemporary compliant mechanism theory, particularly the pseudo-rigid-body model concept (Howell and Midha, 1994), to overcome all of these difficulties.

The examples of bistable MEMS presented in this paper demonstrate how bistable mechanisms may be designed to create more complex motion than has previously been possible for bistable micro-machines. In addition, testing has demonstrated the repeatability of the devices’ equilibrium positions. The mechanisms will be presented by reviewing the behavior of general bistable mechanisms, considering the general mechanism class used in these designs, and describing the testing performed to characterize their bistable behavior.

A BRIEF REVIEW OF BISTABLE MECHANISMS

The nature of mechanism stability may be illustrated using the well-known ball-on-the-hill analogy, illustrated in Fig. 1. In this figure, positions (a) and (c) represent stable equilibrium positions. If the ball is moved a small distance from one of these positions, gravity acts as a restoring force to return the ball to the stable position. However, position (b) is an unstable

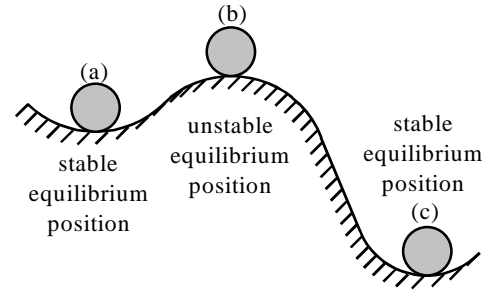


Figure 1: The ball-on-the-hill analogy.

equilibrium position. While the ball will remain at this point without any external restraining force, the slightest disturbance will cause it to move into one of the two stable positions. Therefore, the ball will always be found in one of its two stable positions unless some external force constrains its motions (Timoshenko and Young, 1951; Ginsberg and Genin, 1984).

To move the ball from position (a) to position (c), a force must push the ball up toward position (b). The maximum force required to push the ball will occur at the inflection point in the curve of the hill. This maximum force is called the “critical force” or, if a moment is inducing motion, the “critical moment” (Opdahl et al., 1998). When the ball reaches position (b), a small force applied in the direction of position (c) will cause the ball to move rapidly toward position (c). This quick change to the stable position is called “snapping.”

The ball-on-the-hill analogy may be applied to mechanisms using the Lagrange-Dirichlet theorem, which states that, for an isolated system, “when the potential energy . . . has a minimum for an equilibrium position, the equilibrium position is stable” (Leipholtz, 1970; Lagrange, 1788). Because potential energy minima or maxima for mechanisms correspond to equilibrium positions, a mechanism will be stable in positions where its potential energy curve has a relative minimum (Opdahl et al., 1998). This fact may be used in analysis of the stable states of a mechanism as well as synthesis for new bistable mechanisms.

Compliant Bistable Mechanisms

The potential energy curve will only exhibit local minima if the mechanism has some way to store and release energy during its motion. Many macro-bistable mechanisms use linear springs to store this energy. However, micro-mechanisms require a form of energy storage which can be easily fabricated using standard micromachining techniques. Compliant mechanisms provide an excellent way to satisfy these requirements. The flexible segments in compliant mechanisms store energy as they deflect, and these segments can be easily fabricated using surface micromachining. In this way, the mechanism gains both motion and energy storage from the same compliant segments. Compliant MEMS can also be designed to require no post-fabri-

1. Descriptive titles or acronyms were considered too unwieldy to use conveniently. Instead, the name “Young” was chosen because of the authors’ affiliation with Brigham Young University.

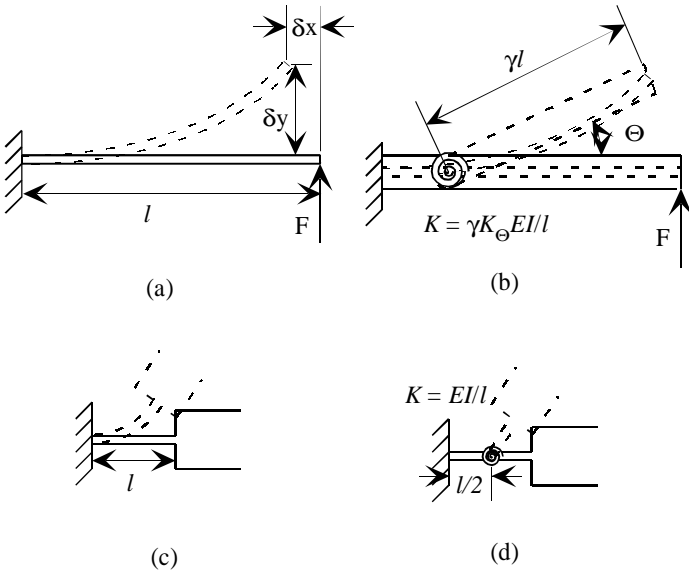


Figure 2: The pseudo-rigid-body model of two compliant segments. The equations giving the model torsional spring constants are written beside each model. γ and K_{Θ} are model constants given by Howell and Midha (1995).

cation assembly (Ananthasuresh and Kota, 1996), one of the reasons that many researchers already use flexible segments in a wide variety of MEMS devices.

Often, however, such flexible segments are limited to very small deflections during mechanism motion. This is because small deflections can easily be predicted using common linear beam-deflection equations. If larger deflections and more complex motion are required, then complex, nonlinear differential equations must be solved to accurately predict the motion of these beams. The solutions to these equations usually involve elliptic integrals (Frisch-Fay, 1962). Consider, for example, the end-loaded cantilever beam shown in Fig. 2a. As long as the deflection, δy , is small, the beam deflection can be approximated with the classic equation

$$\delta y = \frac{FL^3}{3EI} \quad (1)$$

where F is the force applied, L is the length of the beam, and E and I are Young's modulus and the moment of inertia, respectively, of the beam. On the other hand, as δy becomes larger, the error inherent in this approximation grows. Note also that the classical beam equations predict the x -deflection, δx , to be zero. For large deflections, this approximation is obviously untrue. Instead, the deflections δy and δx must be found using elliptic integral solutions which are functions of the load and beam geometry (Bisshopp and Drucker, 1946).

To include the solutions to these elliptic integral equations

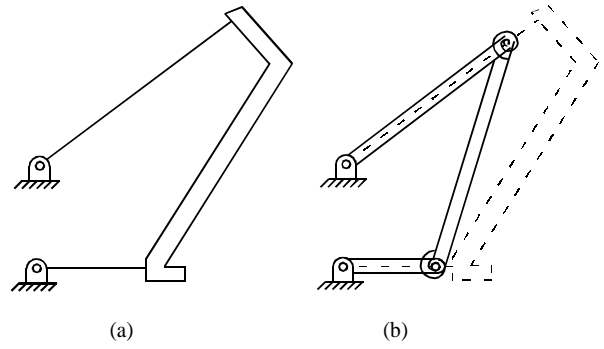


Figure 3: A compliant bistable mechanism (a) with its corresponding pseudo-rigid-body model (b). This mechanism is a Class I bistable micro-mechanism fabricated as part of this study (mechanism 3-I, see Table 1).

in the design process for the desired bistable mechanism behavior would be tedious and overly complex. Instead, compliant mechanism theory has been developed to predict the non-linear deflections of many different flexible beam types (Howell and Midha, 1994; Howell and Midha, 1995; Derderian et al., 1996; Howell et al., 1996). In this model, flexible segments are modeled as two rigid segments joined by a pin joint. A torsional spring models the stiffness of the compliant segment. The placement of the pin joint, as well as the spring constant of the torsional spring, may be calculated using the model. For example, the flexible beam shown in Fig. 2a may be modeled as shown in Fig. 2b, and the small-length flexural pivot shown in Fig. 2c may be modeled with a pin joint in its center, as shown in Fig. 2d. The placement of the pin joints and the values of the torsional spring constants may be found using various model constants and formulas, as shown in the figure. γ and K_{Θ} have been tabulated for a wide range of loading conditions, but they may be approximated for any material properties as (Howell and Midha, 1995)

$$\begin{aligned} \gamma &\approx 0.85 \\ K_{\Theta} &\approx 2.65 \end{aligned} \quad (2)$$

While the pseudo-rigid-body model may be used to predict the force and motion characteristics of flexible beams, its real power lies in its ability to model compliant mechanisms, including MEMS (Jensen et al., 1997). For illustration, the compliant mechanism shown in Fig. 3a may be modeled as the rigid-body mechanism shown in Fig. 3b. This pseudo-rigid-body model has the same force and motion characteristics as the compliant mechanism, and it may be analyzed using rigid-body kinematics. Thus, the model allows the use of well-known kinematics in the analysis and design of compliant mechanisms.

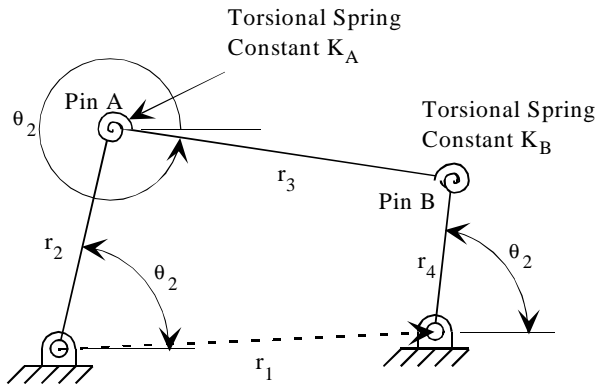


Figure 4: The generic model used to design bistable mechanisms. Pin A and Pin B represent compliant segments according to the pseudo-rigid-body model, with torsional spring constants K_A and K_B

DEFINITION OF YOUNG MECHANISMS

To design compliant bistable planar MEMS, a specific class of mechanisms was defined, known as Young mechanisms. A Young mechanism is one that:

- Has two revolute joints, and, therefore, two links, where a link is defined as the continuum between two rigid-body joints (Midha et al., 1994)
- Has two compliant segments, both part of the same link
- Has a pseudo-rigid-body model which resembles a four-bar mechanism.

The first and second conditions, taken together, imply that the two pin joints are connected with one completely rigid link, while the other link consists of two compliant segments and one or more rigid segments. A general pseudo-rigid-body model of a Young mechanism is shown in Fig. 4. In this model, the two revolute joints are connected to ground, while Pin A and Pin B represent compliant segments modeled by the pseudo-rigid-body model.

Young mechanisms make sense for MEMS for several reasons. For example, pin joints connected to the substrate (ground) can easily be fabricated with two layers of polysilicon, but true pin joints connecting two moving links require more layers. Also, the two pin joints help the mechanism to achieve larger motion, in general, by reducing the stress in the compliant segments. In addition, the two compliant segments give the mechanism the energy storage elements it needs for bistable behavior. Figure 3a illustrates an example of a Young mechanism.

Three main classes of Young mechanisms may be defined, depending on the type of compliant segments used. These are:

- Class I: Both compliant segments are fixed-pinned segments like the one shown in Fig. 2a.

- Class II: One compliant segment is a fixed-pinned segment, and the other is a small-length flexural pivot like the one shown in Fig. 2c.
- Class III: Both compliant segments are small-length flexural pivots.

Classes I and II have been used in this study for bistable MEMS. No mechanisms of Class III were designed because the stresses for the small-length flexural pivots usually exceeded the strength of polysilicon.

A unique Young mechanism of Class I may be described using the seven parameters r_1 , r_2 , r_4 , θ_{20} , θ_{40} , I_2 , and I_4 , where each parameter is defined as:

- r_1 - the distance between the centers of the pin joints.
- r_2 - the length of the largest side-link of the pseudo-rigid-body model. The length l_2 of the associated compliant fixed-pinned segment may be found from the equation

$$l_2 = \frac{r_2}{\gamma} \quad (3)$$

where γ is given in Eq. (2).

- r_4 - the length of the shortest side-link of the pseudo-rigid-body model. The length l_4 of the associated compliant fixed-pinned segment may be found using the same method used to find l_2 .
- θ_{20} - the initial value of θ_2 (defined in Fig. 4) at the undeflected position.
- θ_{40} - the initial value of θ_4 (defined in Fig. 4) at the undeflected position. An alternate approach to define the mechanism would be to specify the value of r_3 rather than one of the two initial angles. However, while r_3 describes the length of the third link in the pseudo-rigid-body model, it has little physical significance in the actual compliant mechanism. In addition, if only one angle is specified, the mechanism could take either the leading or the lagging form based on the link lengths, so that the definition of the mechanism would be less precise.
- I_2 - the area moment of inertia of the flexible segment associated with link 2. For a rectangular cross-section, like those used in this paper,

$$I = \frac{ht^3}{12} \quad (4)$$

where h is the height of the beam (out of the plane of motion) and t is the segment's thickness (within the plane of motion).

- I_4 - the area moment of inertia of the flexible segment associated with link 4. It is given by Eq. (4).

Given these parameters and the material's Young's modulus, the values of the torsional spring constants may be calculated from

the equations

$$K_A = \gamma K_\Theta \frac{EI_2}{l_2} \quad (5)$$

$$K_B = \gamma K_\Theta \frac{EI_4}{l_4} \quad (6)$$

where γ and K_Θ are given in Eq. (2).

Similar parameters are required to define mechanisms of Class II, but an additional variable is needed to define the length of the small-length flexural pivot. The parameters defining a Class II mechanism are:

- $r_1, r_4, \theta_{20}, \theta_{40}, l_4$ - same as for Class I.
- r_2 - the length of pseudo-link 2, defined as the distance from the pin joint to the center of the small-length flexural pivot. No associated value of l_2 may be defined.
- I_2 - the area moment of inertia of the small-length flexural pivot, given by Eq. (4).
- l_s - length of the small-length flexural pivot.

Spring constant K_B is the same as for Class I, but K_A must be found from the equation

$$K_A = \frac{EI_2}{l_s} \quad (7)$$

The Design of Bistable Young Mechanisms

To design bistable Young mechanisms, equations must be used which relate the motion and potential energy of the mechanism. The motion of the model shown in Fig. 4 may be found as a function of θ_2 using rigid-body kinematics. Equations and a description of the process used to analyze the motion of this mechanism may be found in any kinematics textbook (for example, Paul, 1979; Erdman and Sandor, 1997). The potential energy equation may be found by summing the energy stored in the two torsional springs:

$$V = \frac{1}{2}(K_A \psi_A^2 + K_B \psi_B^2) \quad (8)$$

where V is the potential energy, K_A and K_B are the torsional spring constants, and ψ_A and ψ_B are the relative deflections of the torsional springs. These are given by

$$\begin{aligned} \psi_A &= (\theta_2 - \theta_{20}) - (\theta_3 - \theta_{30}) \\ \psi_B &= (\theta_4 - \theta_{40}) - (\theta_3 - \theta_{30}) \end{aligned} \quad (9)$$

where the "0" subscript denotes the initial (undeflected) value of each angle. The minima of Eq. (8) may be found by locating zeroes of the first derivative of V where the second derivative is

positive. The first derivative of V with respect to θ_2 is

$$\frac{dV}{d\theta_2} = K_A \psi_A (1 - h_{32}) + K_B \psi_B (h_{42} - h_{32}) \quad (10)$$

where h_{32} and h_{42} are the kinematic coefficients (Paul, 1979)

$$h_{32} = \frac{d\theta_3}{d\theta_2} = \frac{r_2 \sin(\theta_4 - \theta_2)}{r_3 \sin(\theta_3 - \theta_4)} \quad (11)$$

$$h_{42} = \frac{d\theta_4}{d\theta_2} = \frac{r_2 \sin(\theta_3 - \theta_2)}{r_4 \sin(\theta_4 - \theta_3)} \quad (12)$$

The second derivative of potential energy is

$$\begin{aligned} \frac{d^2V}{d\theta_2^2} &= K_A (1 - 2h_{32} + h_{32}^2 - \psi_A h'_{32}) \\ &+ K_B [h_{42}^2 - 2h_{42}h_{32} + h_{32}^2 + \psi_B (h'_{42} - h'_{32})] \end{aligned} \quad (13)$$

where

$$h'_{32} = \frac{dh_{32}}{d\theta_2} = \frac{r_2}{r_3} \left[\frac{\cos(\theta_4 - \theta_2)}{\sin(\theta_3 - \theta_4)} (h_{42} - 1) - \frac{\sin(\theta_4 - \theta_2) \cos(\theta_3 - \theta_4)}{\sin^2(\theta_3 - \theta_4)} (h_{32} - h_{42}) \right] \quad (14)$$

$$h'_{42} = \frac{dh_{42}}{d\theta_2} = \frac{r_2}{r_4} \left[\frac{\cos(\theta_3 - \theta_2)}{\sin(\theta_3 - \theta_4)} (h_{32} - 1) - \frac{\sin(\theta_3 - \theta_2) \cos(\theta_3 - \theta_4)}{\sin^2(\theta_3 - \theta_4)} (h_{32} - h_{42}) \right] \quad (15)$$

Any value of θ_2 for which Eq. (10) is zero and Eq. (13) is positive identifies a relative minimum of potential energy, and, thus, a stable equilibrium position.

The maximum nominal stress in the compliant segment during motion is another important quantity to consider. Compliant mechanism theory can be used to find this stress from the maximum angular deflection of each segment, $\psi_{A,max}$ and $\psi_{B,max}$. For either compliant segment, the maximum nominal stress may be approximated with the classical stress equation

$$\sigma_{0max} = \frac{M_{max}c}{I} \quad (16)$$

where M_{max} may be approximated, using the pseudo-rigid-body model as the product of K and ψ_{max} . Assuming a rectangular

cross-section,

$$\sigma_{0max} = \frac{6K\psi_{max}}{ht^2} \quad (17)$$

where h is the height of the compliant beam (the dimension out of the plane of motion) and t is its thickness (the dimension within the plane of motion). This nominal stress is the stress calculated without taking stress concentrations into account. It may be used by comparing the nominal stress in the segment to the nominal stress at fracture of previously-tested devices with similar stress concentrations.

To design the mechanisms presented in this paper, the seven (Class I) or eight (Class II) parameters described above were varied to find mechanism configurations with two stable positions, as determined by the potential energy equation, without exceeding the polysilicon strength during motion. To avoid fracture, a maximum strain, equal to the ratio of ultimate strength to Young's modulus, S_{UT}/E , was specified to be 1.05×10^{-2} . This value was determined from prior experience in the design of compliant micro-mechanisms.

This design process was used to design a total of fifteen bistable micro-mechanism configurations, seven of Class I and

eight of Class II. Each mechanism was identified by a number from one to fifteen. The defining parameters for all fifteen mechanism configurations are listed in Table 1. Each mechanism's class is designated by the roman numeral following the mechanism's identifying number. To illustrate the design process, one of these mechanisms, mechanism number 5-II, will be studied in more detail.

A Bistable Mechanism Example

Mechanism 5 is a Class II mechanism, with one small-length flexural pivot and one fixed-pinned segment, as illustrated in Fig. 5a. The design parameters for this mechanism are listed in Table 1. These parameters define the pseudo-rigid-body model shown in Fig. 5b. Using the design parameters listed in Table 1, the potential energy curve through the mechanism's motion may be generated using Eq. (8). This curve is shown as a function of θ_2 in Fig. 6. The two relative minima on this curve represent the two stable positions of the mechanism. These minima occur at $\theta_2 = \theta_{20} = 83^\circ$ and $\theta_2 = 7^\circ$. Therefore, the angular deflection of the second link between the two stable positions is approximately 76° . At each point, the first derivative of potential energy, given in Eq. (10), is zero, and the second derivative, given in Eq. (13), is positive.

Table 1: Design parameters for the fifteen mechanisms. Each mechanism's class is given by the roman numeral following the dash in the mechanism number.

Mech. No.	$r_1, \mu\text{m}$	$r_2, \mu\text{m}$	$r_4, \mu\text{m}$	θ_{20}	θ_{40}	$I_2, \mu\text{m}^4$	$I_4, \mu\text{m}^4$	$I_s, \mu\text{m}$
1-I	120	480	108	130°	40°	4.5	4.5	
2-I	120	216	120	130°	90°	4.5	4.5	
3-I	120	236	109	130°	90°	4.5	4.5	
4-II	100	295	364	83°	53°	7.88	4.5	26
5-II	100	250	250	83°	53°	4.5	4.5	26
6-II	100	200	300	70°	46°	7.88	4.5	33
7-II	100	300	400	90°	45°	7.88	4.5	30
8-II	100	300	400	90°	45°	4.5	4.5	30
9-I	120	360	78	140°	50°	4.5	4.5	
10-I	100	404	144	130°	58°	4.5	4.5	
11-I	100	404	128	130°	58°	4.5	4.5	
12-II	100	80	200	40°	15°	7.88	4.5	9
13-II	100	80	200	40°	15°	7.88	4.5	9
14-II	100	130	200	30°	15°	4.5	4.5	13
15-I	100	250	120	120°	200°	4.5	4.5	

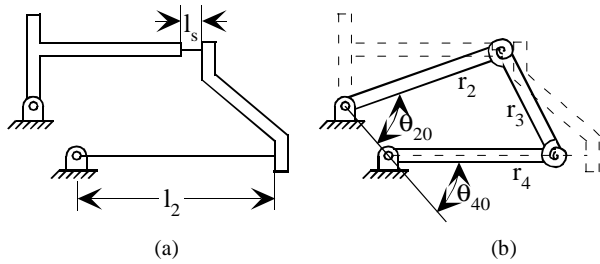


Figure 5: An illustration of mechanism 5-II (a) with its pseudo-rigid-body model (b).

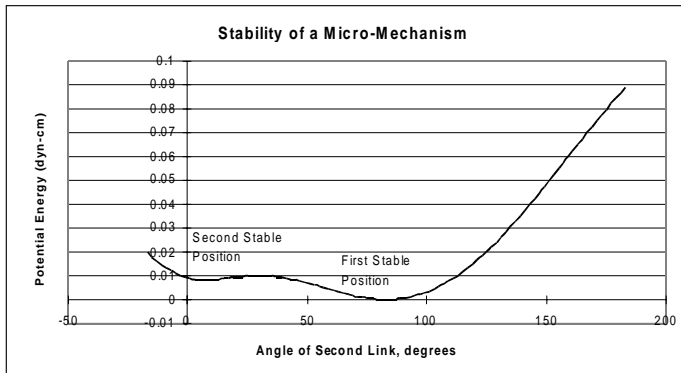


Figure 6: The potential energy curve of mechanism five as a function of θ_2

The maximum strain in each compliant segment may be calculated using Eq. (17). This strain is 1.02×10^{-2} for the small-length flexural pivot and 5.74×10^{-3} for the fixed-pinned segment. As stated earlier, fracture is expected when the ultimate strain is reached at 1.05×10^{-2} .

MECHANISM FABRICATION AND TESTING

Each of the fifteen mechanism configurations was fabricated using the Multi-User MEMS Process (MUMPS) at MCNC. This process allows the designer to use two released layers of polysilicon. For all cases, the mechanisms were fabricated from the first layer, with a thickness of $2.0 \mu\text{m}$. In addition, the “stacked polysilicon” method described by Comtois and Bright (1995) was used to make some of the small-length flexural pivots as thick as both layers, or $3.5 \mu\text{m}$ thick. The pin joints fixed to ground were fabricated as shown in Fig. 7, with a disk formed from the first layer of polysilicon and a post formed by the second layer. The mechanisms were released at the BYU Integrated Microelectronics Laboratory and were tested by displacing them with probes. Figure 8 shows a SEM photograph of an example mechanism from Class I (mechanism 3-I) and another from Class II (mechanism 5-II).

Eleven of the mechanism configurations fabricated demon-

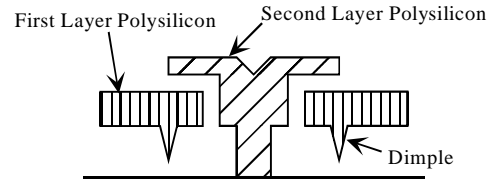


Figure 7: A cross-section of the pin joints fixed to the substrate. A disk is formed from the first layer of polysilicon, with a post formed from the second layer of polysilicon.

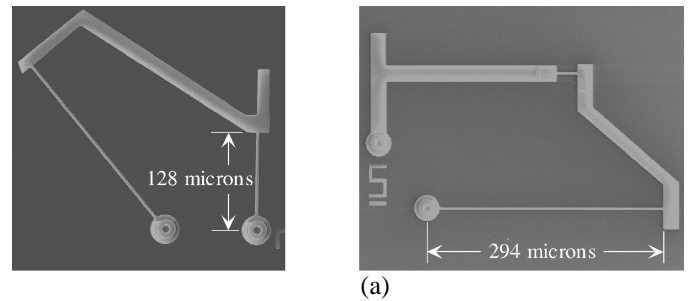


Figure 8: Scanning electron microscope (SEM) photographs of two bistable micro-mechanisms. One dimension is given to provide an idea of the mechanism’s scale.

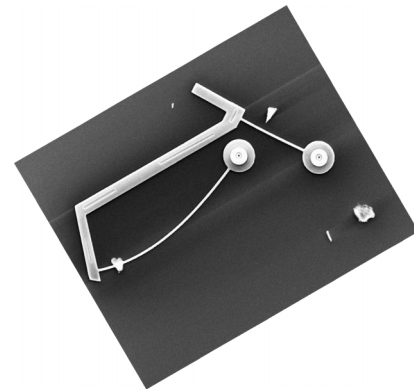


Figure 9: Mechanism 3-I in its second stable position.

strated bistable behavior by snapping between the two stable states. Figures 9 and 10 show microscope images of two example mechanisms in the second stable position. In the figures, note the large, non-linear deflections in the compliant segments. Note also that one of the compliant segments is still deflected in the second stable position, indicating that some energy is stored in that state. Despite this stored energy, the mechanism is at a local minimum of potential energy. In other words, while the second stable position does not represent an

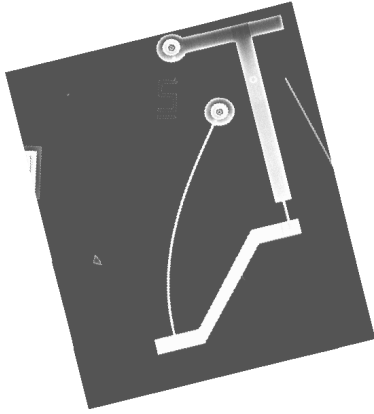


Figure 10: Mechanism 5-II in its second stable position.

absolute minimum of potential energy (i.e., the potential energy is not zero), it is a local minimum because any small deviation from that position requires more energy to be put into the mechanism. Figure 6 illustrates this point for mechanism 5-II. The pictures showing the second stable position were taken by displacing the mechanisms until they reached their unstable states, after which they snapped into the positions shown. This successful snapping behavior represents the first time planar MEMS have shown bistable behavior without buckling.

The repeatability of each stable position was measured by recording the angle between a reference line and a rigid part of each mechanism. For example, on mechanisms of Class II, the angle ABC, shown in Fig. 11, was measured when the mechanism was in each stable position. This measurement allows determination of the change in θ_2 for the two stable

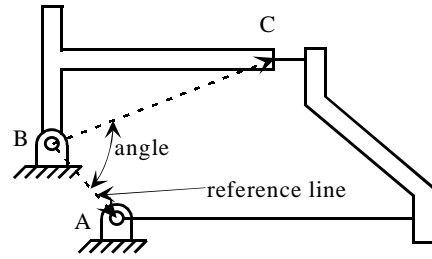


Figure 11: The angle measured to determine the repeatability of mechanism five's stable positions

positions. For mechanisms of Class I, the angle between the line joining the pin joints and the rigid coupler link was measured. This angle allows determination of the change in θ_3 for the two stable positions.

The angle was measured in each case over several cycles of snapping. The measurement was made using computer analysis of video images. The standard deviation of the angles measured in each position was then used as an indication of the variation in position for that stable state. Of the eleven configurations which successfully snapped between positions, only eight snapped enough times before fracture to make a good measurement of the variability in the stable position. The standard deviations of the angles for these eight mechanism configurations are listed in Table 2, along with the difference between the means of the angles measured at each position. The difference in the means is presented to allow comparison between the angular difference between stable states and the variation of position at each stable state. The predicted angular difference between the stable positions is also shown. Many of the mechanisms showed a very low standard deviation, indicating a high level of repeatability in the stable positions.

Table 2: The standard deviation of angles measured at stable positions. Position 1 is the undeflected stable position; Position 2 is the other stable position.

Mechanism	Mean Angular Difference	Samples at Pos. 1	St. Dev., Pos. 1	Samples at Pos. 2	St. Dev., Pos. 2	Predicted Angular Difference
2-I	0.849 rad	3	0.053 rad	4	0.099 rad	0.958 rad
3-I	0.909 rad	7	0.038 rad	6	0.098 rad	1.09 rad
5-II	1.30 rad	8	0.020 rad	7	0.0079 rad	1.36 rad
10-I	1.10 rad	7	0.074 rad	3	0.079 rad	1.33 rad
11-I	1.18 rad	6	0.034 rad	6	0.025 rad	1.36 rad
12-II	0.457 rad	10	0.068 rad	10	0.027 rad	0.349 rad
13-II	0.449 rad	18	0.056 rad	20	0.043 rad	0.349 rad
14-II	0.308 rad	12	0.064 rad	14	0.061 rad	0.332 rad

However, in most cases, the measured angular difference is less than the predicted angular difference. This is because friction between the mechanism and the substrate exceeds the restoring force for small deviations around the stable position.

While many of the mechanisms showed good bistable behavior, several of the mechanisms either failed to snap or else fractured after snapping once or twice. This is most likely due to high frictional forces caused by rubbing against the substrate. The frictional forces could overcome the mechanism's restoring force, causing the mechanism not to snap into a stable position. Methods of decreasing the friction between the mechanism and the substrate are currently being studied to improve the performance of these mechanisms.

CONCLUSION

The properties of a class of planar compliant mechanisms, called Young mechanisms, have been investigated. These mechanisms have some qualities that make them ideal for MEMS. The mechanisms consist of two links, joined by two pin joints. One link is rigid; the other contains two compliant segments. This configuration is useful for MEMS because the pin joints, if they are attached to the substrate, can be fabricated using only two released layers of polysilicon, and the compliant segments can easily be fabricated in only one layer. This class of mechanisms is especially important in the design of bistable MEMS. The pin joints generally allow a high degree of mobility without high stress, and the compliant segments allow motion while storing and releasing the energy needed to make the mechanism bistable.

Young mechanisms have been further divided into three classes, depending on the type of compliant segments used. Class I mechanisms have two fixed-pinned compliant segments, Class II mechanisms consist of one fixed-pinned segment and one small-length flexural pivot, and Class III mechanisms have two small-length flexural pivots. Young mechanisms of Class I or Class II can be uniquely described using seven or eight parameters. Using compliant mechanism theory, the motion and potential energy characteristics of a mechanism can be found if these parameters are known.

Therefore, several configurations of Young mechanisms have been designed to achieve bistable behavior in MEMS. They were designed by varying the mechanism's defining parameters to find configurations with two stable states, while keeping stress low. These configurations were fabricated and tested, and several of them demonstrated the expected bistable behavior. These mechanisms are the first MEMS to snap between stable positions within their plane of fabrication.

The test mechanisms showed a high degree of repeatability in the stable positions. These results show that the mechanisms have great promise for use in a variety of applications, including mechanical switching, non-volatile memory, and microfluidic valves. Future work to be done in this area includes fatigue testing, integration of actuation methods for the mechanisms,

investigation of the dynamic response of the mechanisms, and producing better synthesis methods which will allow a designer to more easily create new bistable MEMS.

ACKNOWLEDGMENTS

Special thanks is given to Brian Christensen, who gathered much of the data on the repeatability of the stable positions. The assistance of Rebecca Cragun is also gratefully acknowledged. This material is based upon work supported under a National Science Foundation Graduate Fellowship and a National Science Foundation Career Award No. DMI-9624574.

REFERENCES

- Ananthasuresh, G.K. and Kota, S., 1996, "The Role of Compliance in the Design of MEMS," *Proceedings of the 1996 ASME Design Engineering Technical Conferences*, 96-DETC/MECH-1309.
- Bisshopp, K.E. and Drucker, D.C., 1945, "Large Deflection of Cantilever Beams," *Quarterly of Applied Mathematics*, Vol. 3, No. 3, pp. 272-275.
- Comtois, J.H. and Bright, V.M., 1995, "Design Techniques for Surface-Micromachining MEMS Processes," *SPIE*, Vol. 2639, pp. 211-222.
- Derderian, J.M., Howell, L.L., Murphy, M.D., Lyon, S.M., and Pack, S.D., 1996, "Compliant Parallel-Guiding Mechanisms," *Proceedings of the 1996 ASME Design Engineering Technical Conferences*, 96-DETC/MECH-1208.
- Erdman, A.G. and Sandor, G.N., 1997, *Mechanism Design: Analysis and Synthesis*, Vol. 1, 3rd Ed., Prentice Hall, New Jersey.
- Frisch-Fay, R., 1962, *Flexible Bars*, Butterworth, Washington, D.C.
- Ginsberg, J.H. and Genin, J., 1984, *Statics and Dynamics, Combined Version*, John Wiley & Sons, New York.
- Hälg, B., 1990, "On A Nonvolatile Memory Cell Based on Micro-electro-mechanics," *IEEE Micro Electro Mechanical Systems 1990*, pp. 172-176.
- Howell, L.L. and Midha, A., 1994, "A Method for the Design of Compliant Mechanisms with Small-Length Flexural Pivots," *ASME Journal of Mechanical Design*, Vol. 116, No. 1, pp. 280-290.
- Howell, L.L. and Midha, A., 1995, "Parametric Deflection Approximations for End-Loaded, Large-Deflection Beams in Compliant Mechanisms," *ASME Journal of Mechanical Design*, Vol. 117, No. 1, pp. 156-165.
- Howell, L.L., Midha, A., and Norton, T.W., 1996, "Evaluation of Equivalent Spring Stiffness for Use in a Pseudo-Rigid-Body Model of Large-Deflection Compliant Mechanisms," *ASME Journal of Mechanical Design*, Vol. 118, No. 1, pp. 126-131.
- Jensen, B.D., Howell, L.L., Gunyan, D.B., and Salmon, L.G., 1997, "The Design and Analysis of Compliant MEMS Using the Pseudo-Rigid-Body Model," *Microelectromechanical Systems*

(MEMS) 1997, at the 1997 ASME International Mechanical Engineering Congress and Exposition, DSC-Vol. 62, pp. 119-126.

Lagrange, J.L., 1788, *Mecanique Analytique*, Vol. 1, Pt.1, Sec. 3, Art 5, published 1853 by Mallet-Bachelier, Paris.

Leipholz, H., 1970, *Stability Theory*, Academic Press, New York and London.

Matoba, H., Ishikawa, T., Kim, C., and Muller, R.S., 1994, "A Bistable Snapping Mechanism," *IEEE Micro Electro Mechanical Systems 1994*, pp. 45-50.

Midha, A., Norton, T.W., and Howell, L.L., 1994, "On the Nomenclature, Classification, and Abstractions of Compliant Mechanisms," *ASME Journal of Mechanical Design*, Vol. 116, No. 1, pp. 270-279.

Opdahl, P.G., 1996, "Modeling and Analysis of Compliant Bistable Mechanisms Using the Pseudo-Rigid-Body Model," M.S. Thesis, Brigham Young University, Provo, Utah.

Opdahl, P.G., Jensen, B.J., and Howell, L.L., 1998, "An Investigation into Compliant Bistable Mechanisms," *Proceedings of the 1998 ASME Design Engineering Technical Conferences*, DETC98/MECH-5914.

Paul, B., 1979, *Kinematics and Dynamics of Planar Machinery*, Prentice-Hall, Inc., Englewood Cliffs, New Jersey.

Timoshenko, S. and Young, D.H., 1951, *Engineering Mechanics 3rd Ed.*, McGraw-Hill Book Company, Inc., New York.

Wagner, B., Quenzer, H.J., Hoershelmann, S., Lisec, T., and Juerss, M., 1996, "Bistable Microvalve with Pneumatically Coupled Membranes," *Proceedings of IEEE Micro Electro Mechanical Systems 1996*, p. 384-388.